Precision Passive Mechanical Alignment of Wafers

Alexander H. Slocum and Alexis C. Weber

Abstract—A passive mechanical wafer alignment technique, capable of micron and better alignment accuracy, was developed, fabricated and tested. This technique is based on the principle of elastic averaging: It uses mating pyramid (convex) and groove (concave) elements, which have been previously patterned on the wafers, to passively align wafers to each other as they are stacked. The concave and convex elements were micro machined on 4-in (100) silicon wafers using wet anisotropic (KOH) etching and deep reactive ion etching. Submicron repeatability and accuracy on the order of one micron were shown through testing. Repeatability and accuracy were also measured as a function of the number of engaged elements. Submicrometer repeatability was achieved with as little as eight mating elements. Potential applications of this technique are precision alignment for bonding of multiwafer MEMS devices and three-dimensional (3-D) inter-connect integrated circuits (ICs), as well as one-step alignment for simultaneous bonding of multiple wafer stacks. Future work will focus on minimizing the size of the elements. [920]

Index Terms—Elastic averaging, kinematic coupling, wafer alignment, wafer bonding.

I. INTRODUCTION

SUBMICRON alignment for wafer bonding applications has become a major limitation in the development of multi-wafer MEMS devices and three-dimensional (3-D) interconnects [1], [2]. Most wafer alignment is done by mechanically positioning one wafer with respect to another using optical measurement techniques, but the large structural loop[1] makes alignment better than 1 μm difficult, and multiwafer stacks must be assembled one at a time. In addition, for multiwafer assemblies, when assembled one at a time, alternating curvatures have the potential to cause subsequently added wafers to be overstressed or deformed. Passive alignment has been used extensively for alignment of optical fibers in MOEMS [3]–[5], and has been used in setups for "rough" wafer-to-wafer alignment [6], and in MEMS packaging applications [7]. Capillary forces at the wafer-air interface between hydrophobic features patterned on wafers can align two wafers to each other to the micron level [8], but would be impractical for a stack of wafers.

This background gives rise to the hypothesis that there must be a way to passively and simultaneously align multiple wafers. Accordingly, this paper describes a methodology used to passively align wafers using the principle of elastic averaging.

The authors are with the Precision Engineering Research Group, Department of Mechanical Engineering, Massachusetts Institute of Technology, Cambridge, MA 02139 USA (e-mail: slocum@mit.edu).

[1]The structural loop is the complete load path through the system, and hence when optically aligning wafers, the structural loop includes the path from one wafer, through the chuck and the machine to the other wafer.
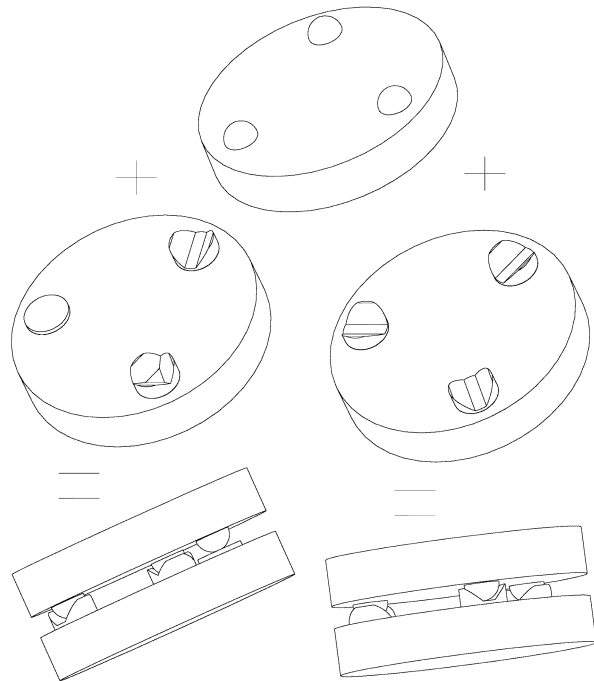

Fig. 1. An object with three hemispheres (top-center) can be deterministically and repeatably coupled to another object with either three v-grooves (middle-right) or with a flat, a v-groove and a trihedral feature (middle left) to create a deterministic kinematic coupling (bottom left and bottom right).

II. PRECISION ALIGNMENT PRINCIPALS

The design and manufacture of precision instruments and machines has a rich history that emphasized the use of fundamental principles of alignment in order to continually create machines more accurate than those available [9]. Two primary alignment techniques come to mind, kinematic and elastic averaging [10]. The former requires a system to be statically determinant: the number of contact points (independent constraints) equals the number of degrees of freedom restrained. The latter assumes the system is grossly over constrained, but each contact element is relatively flexible, and when forces are applied to clamp the system, the elements deform elastically and errors average.

There are many references to instruments designed as kinematic, or "exact constraint" systems [11]–[13]. These often use a kinematic coupling between the elements. Fig. 1 shows two such variants: a three-groove kinematic coupling, which was used by Maxwell to align components in his experiments with light, and three hemispheres mated against a flat plat, a trihedral socket, and a v-groove that pointed toward the socket which was used by Lord Kelvin. The detailed analysis methods for creating kinematic couplings between components are now well known [14], [15] where even factors such as friction between surfaces can be overcome with the use of flexural elements to provide compliance in the direction of friction forces, while maintaining high normal stiffness [16].

The principle of *elastic averaging* states that to accurately locate two surfaces and support a large load, there should be a large number of contact points spread out over a broad region. Examples include curvic or Hirth couplings, which use meshed gear teeth (of different forms respectively) to form a coupling. The teeth are clamped together with a very large preload. This mechanism is commonly used for indexing tables and indexing tool turrets. A more common example is that of a *wiffle tree* which is the structure that provides support to a windshield wiper. Fig. 2 shows the principle as it would be used to allow a single point of loading to apply an even force to 28 devices (e.g., for testing packaged semiconductor devices). An example of the principle of elastic averaging taken to its extreme limit is the structure of the gecko's feet. These animals' feet are covered with hairs, which continue to subdivide at their ends to the microscopic level where they each then can make intimate contact with a surface so Van der Waals forces enable the gecko to stick to smooth surfaces [17].
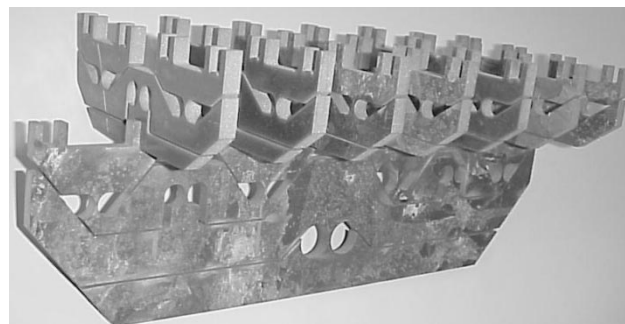
There are few references to instruments where precision alignment is attained by elastic averaging, perhaps because the analysis is often intractable, or perhaps because using this method implies a higher risk associated with an overconstrained system being subject to distortion by assembly forces or environmental factors; however, recently the principle was applied to a new type of shaft coupling [18]. In addition, an interesting elastic averaging effect in silicon was obtained by Han who created "silicon Velcro" that can act as a surface adhesive using thousands of interlocking features [19].
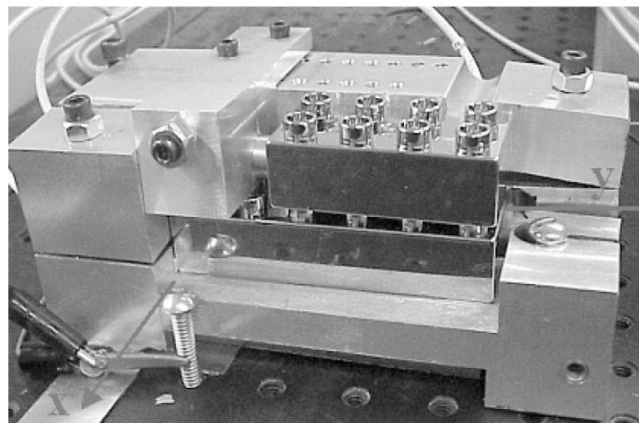
Thus we approached the problem of aligning wafers from the perspective of investigating the possibility of using kinematic or elastic averaging principles, or perhaps even a hybrid system. The first step being a series of experiments to investigate what sort of features might be formed on a wafer to enable an elastic averaging approach. Accordingly, we turned to a very common elastically averaged product used to stack objects together: LEGO blocks (LEGO is a registered trademark of the LEGO Group and LEGO Systems, Inc., Enfield, CT 06083 USA).

III. ELASTIC AVERAGING BENCH LEVEL EXPERIMENT

A series of experiments were performed on LEGO DUPLO blocks (LEGO DUPLO is a registered trademark of the LEGO Group and LEGO Systems, Inc., Enfield, CT 06083 USA) to quantitatively evaluate the repeatability that can be obtained through the principle of elastic averaging. LEGO building blocks have a set of convex features, or primary projections (PP) and concave features, or secondary projections (SP), which are designed to engage with each other. When two blocks are placed on top of each other and then forced together (engaged or preloaded), a small interference fit between the relatively high compliant mating features creates the necessary frictional force to keep the blocks fixed to each other [20].
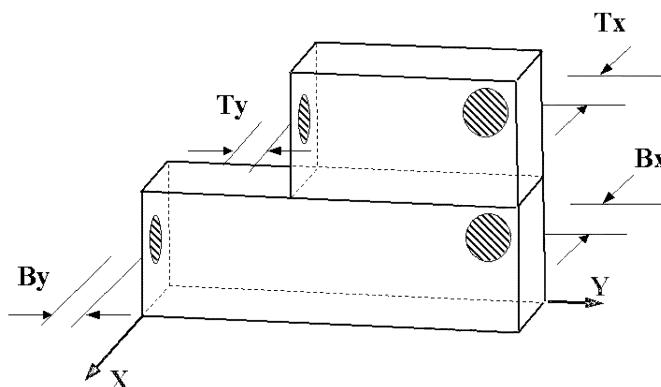
LEGO blocks of 8 and 6 PP were repeatedly assembled to each other. The absolute position of the top and the bottom block was recorded at every assembly cycle. The assembly's repeatability was calculated as the total range of the block's position.[2] This experiment was run on three different setups. First, the position of the blocks was taken with a Coordinate Measurement

[2]The data taken with the capacitive probes was normalized to the average position for each probed face.

Fig. 2.   Example of 3-D Wiffle tree structure.

Fig. 3.   System used for measuring the repeatability of LEGO blocks.

TABLE I
REPEATABILITY (μm) OF 2 BY 4 PP LEGO DUPLO BLOCK

Set-up	Bx	Tx	By	Ty	Bz	Tz
CMM	5	19	5	20	5.3	20.3
Capacitive, using bonded sheet target	4.7	14.5	4.5	27.4	N/A	N/A
Capacitive, using chrome-plated blocks	1.8	3.4	1.2	4.5	N/A	N/A

Fig. 4.   Probe position and target nomenclature used in bench level experiment.

Machine (CMM) but the LEGO blocks were found to be more repeatable than the CMM! In the second setup, a thin aluminum sheet glued to the blocks was used as a target for capacitive probes, but it was difficult to get stability from the adhered sheet. These blocks were finally replaced by chrome-plated blocks in the third setup, as shown in Fig. 3, which also shows the results
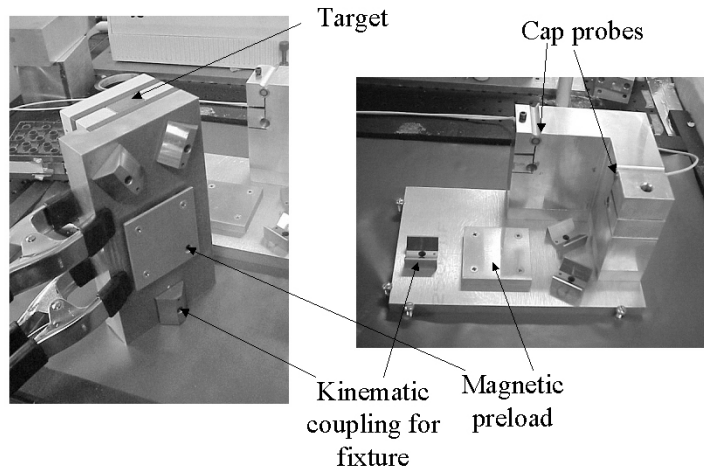
Fig. 5.   Second bench level experiment setup. A LEGO platform is epoxied to a metal base which is kinematically coupled to the measurement fixture. This establishes a baseline repeatability (submicron).
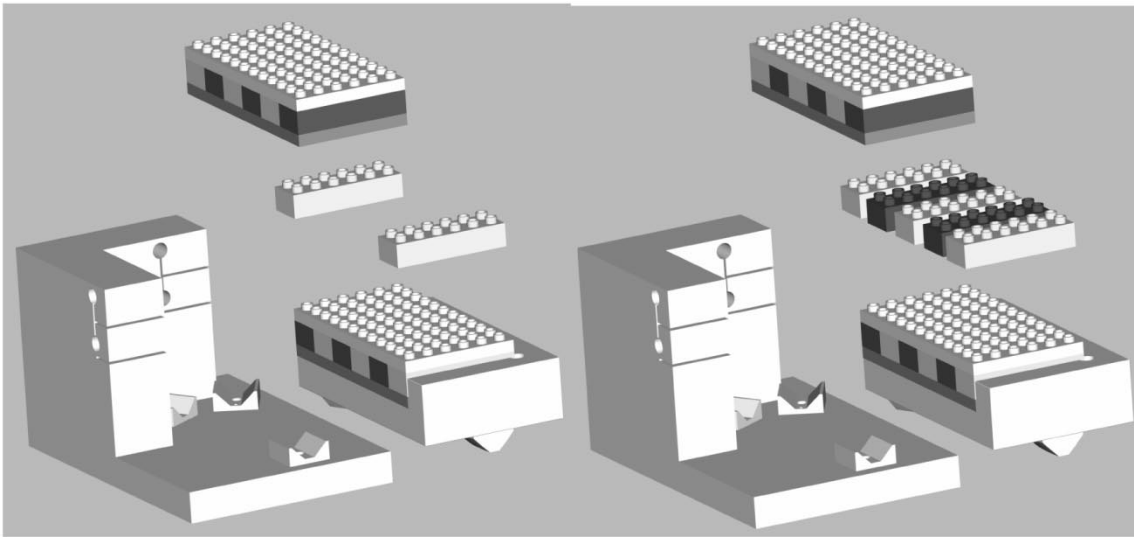

Fig. 6.   Second bench level experiment setup with 72 (24 × 3) contact points (left figure) and 180 (60 × 3) contact points (right figure) between the top LEGO plate and the bottom LEGO plate structures.

TABLE II
REPEATABILITY (μm) OF MEASUREMENT SYSTEM (SECOND BENCH LEVEL EXPERIMENT)

	Bx	By	Tx	Ty
Repeatability (μm)	0.56	0.52	0.23	0.85

of the first experimental attempts. Chrome-plated blocks were used in this experiment to provide a conductive target for the capacitive probes while reducing the error induced in the previous setup by relative movement of the aluminum sheet to the block.

Table I shows the results of the experiment, as defined in Fig. 4, for a 30 cycle assembly-disassembly run. The repeatability of the measurement system itself was determined to be of the order of 0.1 μm. The nonzero repeatability of the bottom block is attributed to creep and thermal growth due to $\pm2°$C variations in the laboratory. It was expected that **Ty** (repeatability of top block in the y direction) be better than **Tx**, (repeatability of top block in the x direction), since repeatability is typically thought to be inversely proportional to the square root of the number of contact points [10], and more contact points lie along the y direction then along the x direction of the blocks. However, this was not the case, and it is believed that

the Abbe error caused by the blocks' aspect ratio, dominates the total error. Thus the relationship between the number of contact points and the magnitude of the error was indistinguishable. Nevertheless, the repeatability values obtained are quite impressive and the overall system provided good insight into how a wafer coupling system should be designed.

A second bench level experiment was developed to evaluate the relationship between the number of contact points and the repeatability of an elastically averaged coupling. The setup used, shown in Fig. 5, allows the number of engaged primary and secondary projections between two monolithic target blocks to be varied. The relatively stiff monolithic blocks, comprised of individual, LEGO blocks[3] that were expoxied together, were assembled repeatedly while recording the top and the bottom blocks'

---

[3]Chrome plated blocks were epoxied in the monolithic blocks and used as targets for the capacitive probes.

TABLE III
REPEATABILITY (μm) OF SECOND BENCH LEVEL EXPERIMENT

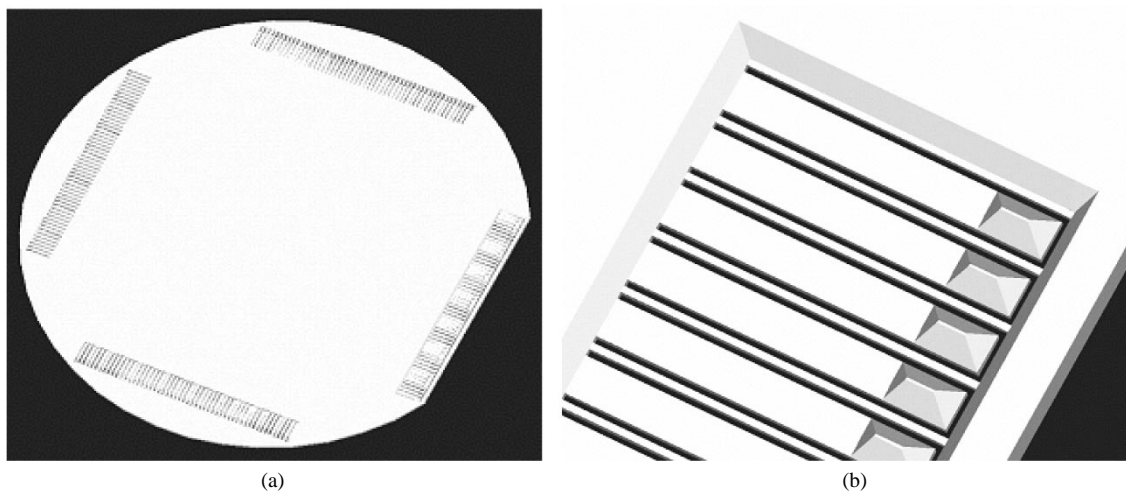| Experiment	X	Y	σ_X	σ_Y
2 Lego blocks (72 contact pts.)	8.15	10.95	2.48	2.76
4 Lego blocks (144 contact pts.)	5.47	6.23	1.27	1.74
5 Lego blocks (180 contact pts.)	2.80	3.59	0.77	1.02

(a) (b)

Fig. 7.   (a) Solid model of the of convex structures. (b) Detail of convex structure.

absolute position. Two to five LEGO blocks, each with 2 by 6 PP were placed between the monolithic blocks to vary the number of contact points by which the monolithic blocks are engaged. Fig. 6 shows the setup with 72 (2 LEGO blocks) and 180 contact points (5 LEGO blocks), respectively.

The fixture used in this experiment, shown in Fig. 5, consists of a base to which the capacitive probes are fixed to by means of flexural clamps, and a detachable plate, to which one of the monolithic block has been epoxied. Both parts of the fixture are coupled to each other by a canoe-ball type[4] three groove kinematic coupling. A two-piece setup is used to allow remote assembly and disassembly of the monolithic blocks.[5]

The detachable plate can be tilted away from the base, which contains the capacitive probes, to a safe distance for block assembly and disassembly. The kinematic coupling allows the detachable plate to return to the original position relative to the base with submicron repeatability. The preload for the kinematic coupling in this experiment is provided by the mass of the top fixture and by two permanent magnets fixed to the top and the bottom parts of the fixture. Submicron repeatability of the measurement system, as shown in Table II, was determined with this setup. The setup was placed in an insulating chamber to reduce errors due to thermal expansion. Table III shows the results of a

[4]Instead of using three balls, three surfaces with local radii of contact of 0.25 m, which were ground on a CNC grinding machine, were used so the stiffness and load capacity (preloadability) of the interface are two orders of magnitude greater than for balls. These surfaces look like the bottom of a canoe, and hence are called *canoe-ball* kinematic couplings, and they typically provide sub micron repeatability even when subject to heavy loads. We use these modular canoe-ball coupling elements in our lab because they are far less likely to be damaged by professors in the lab.

[5]The capacitive probes are spaced less than 1 mm away from the monolithic blocks; the two-piece setup prevents physical contact with the probes which causes unwanted drift in the measurements.

25 cycle assembly–disassembly run varying the number of contact points.

As expected, both repeatability and standard deviation improve as the number of contact points increases. The theory of random errors would indicate that the repeatability of an elastically averaged coupling is inversely proportional to the number of contact points. Although this is not reflected quantitatively, the experimental results clearly show this trend qualitatively.

IV. PASSIVE WAFER ALIGNMENT STRATEGY

Kinematic couplings and elastically averaged systems are well known to the precision macro world, and hence these principles were applied to create a passive mechanical alignment technique that makes use of matching convex and concave wafer integral features. Given that a kinematic coupling ideally requires high precision compound angled surfaces, which are extremely difficult to create in silicon wafers, and given the design development of a new backlash-free spline coupling formed by eleastically deforming interlocking engagement fingers [22], as well as the observations that LEGO construction bricks seem to fit together well, it was hypothesized that the wafer-to-wafer alignment system could be created based on the concept of elastic averaging using a multitude of structures that might otherwise be used in a kinematic coupling.

The concave alignment structures, shown in Fig. 7, consist of eight arrays (two per wafer edge) of 22 KOH-etched pyramid-structures mounted on the tip of cantilever flexures [21]. The convex structures consist of matching arrays of v-trenches (trenches verses grooves because the bottoms are flat) patterned on a boss, shown in Fig. 8. When the two wafers
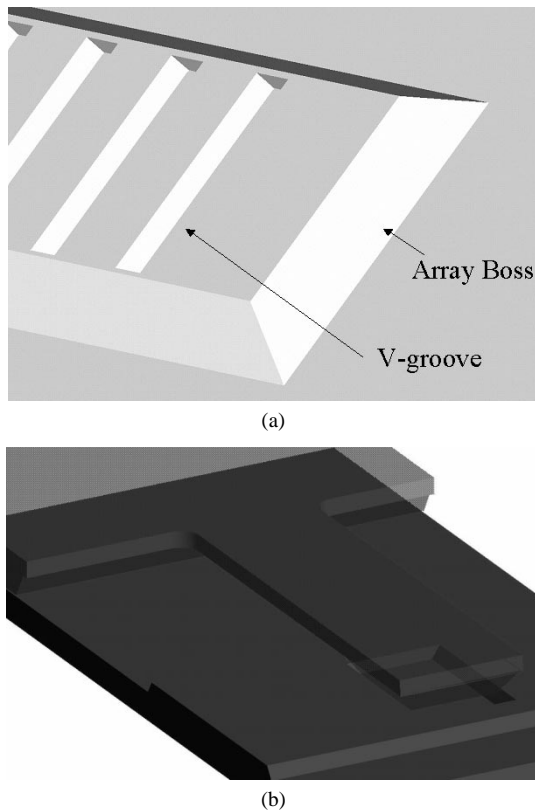
TABLE IV
CONCAVE AND CONVEX ELEMENT FEATURE SIZES

Feature	Mask	Size (μm)
Pit length	M-1	7 000
Pit width	M1	26 000
Pit distance from wafer center line (inner edge)	M-1	7 500
Cantilever length	M-1 M-2	5 260
Cantilever width	M-2	1 400
Cantilever thickness	M-2	200-250
Pyramid size, at the pyramids top	M-1	1 072
Pyramid size, at the pyramids base	M-1	1 450
CCCS outer rectangle	M-1	2 000
V-trench width	F-1	1 142
V-trench length	F-1	1 900

Fig. 8. (a) Solid models illustrating the boss and v-groove arrays of the concave structures and (b) of the assembled structures.

are stacked upon each other, the wafer chuck is tapped lightly[6] in a direction normal to the wafers so the vibration overcomes any friction between the contact interfaces and lets the wafers settle into place. The wafers are then preloaded together and the interface between the v-trenches and the pyramid causes the flexures to bend. The mating structures self-align the wafers achieving an elastic averaging effect as also shown in the assembled state in Fig. 8.

V. DESIGN OF ALIGNMENT FEATURES

Table IV presents the dimensions of both concave and convex features. Both features are sized to minimize wafer intrusion while keeping the cantilever strain below 0.2% for a 150 μm cantilever tip deflection. The pyramids are sized such that a compact convex corner compensating structure (CCCS), shown in Fig. 9 and designed after [23], can be fitted between the pyramids. The CCCS is needed to prevent beveling of the pyramid's convex corners. Generous radii were patterned on the cantilevers' bases during the DRIE step to prevent stress concentration. A halo-mask was used during the DRIE step to shorten the process time and to maintain a constant etch rate throughout the whole wafer.

VI. MICROFABRICATION

Three micron feature size alignment marks were patterned on the wafer front side (for convex feature wafers) and the wafer

---

[6]How much tapping is required is a parameter that was not quantified, but will be the subject of future work to determine repeatability as a function of vibration direction, amplitude and duration.

back side (for concave feature wafers) of 4-inch double-sided polished (100) silicon wafers. The convex features were fabricated with a backside KOH-timed etch, which created a 300-μm-deep pit that defined the cantilever thickness and the pyramid structures. A front-side DRIE released the cantilevers. The concave features were bulk micro-machined through a single timed KOH etch, which thinned out most of the wafer, leaving eight bosses with an equal number of v-trench arrays. Figs. 10 and 11 show the detailed fabrication process for both convex element feature wafers and concave element feature wafers, respectively.

Figs. 12 and 13 show SEM pictures of the convex coupling features and array, as seen from the bottom of the wafer. Note in Figs. 12 and 13, that although CCCS were used to mask this wafer, the convex pyramid corners are beveled. This wafer was purposely overetched during the timed KOH etch to ensure no traces of the CCCS would be present, which could interfere between the convex and the concave features during wafer assembly. Fig. 14 shows a close up view of the boss and v-trenches or concave structures. The alignment marks were patterned with a standard e-beam written mask. The KOH etches of both concave and convex structures, as well as the DRIE steps were patterned using masks made from emulsion transparencies.

VII. TESTING PASSIVE ALIGNMENT FEATURES

Testing of the passive wafer alignment features was done on an Electronics Vision Group™ TBM8™ wafer alignment inspection system, as shown in Fig. 15. Two stacked wafers were mounted on the TBM8™, aligned roughly and tapped lightly on the wafer chuck about 25 mm from the wafers in a direction normal to the wafer plane to help the wafer alignment elements engage and align the wafers. After the top wafer had reached a stable position (i.e., would not move after tapping), the front-to-back side alignment accuracy was determined, by measuring the relative position of the alignment marks on both wafers. The wafer was then removed and put back on many times so repeatability could be determined. Submicron repeatability and accuracy in the order of 1 μm were shown through testing. Table V shows the performance of the measurement system as determined through a "cap test", whereby a wafer
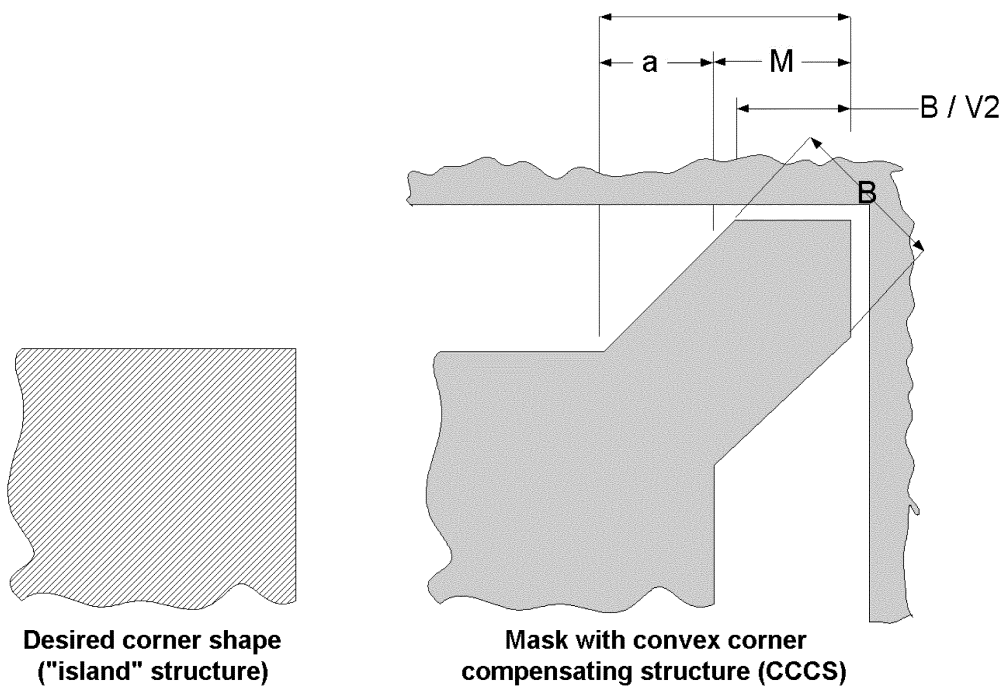
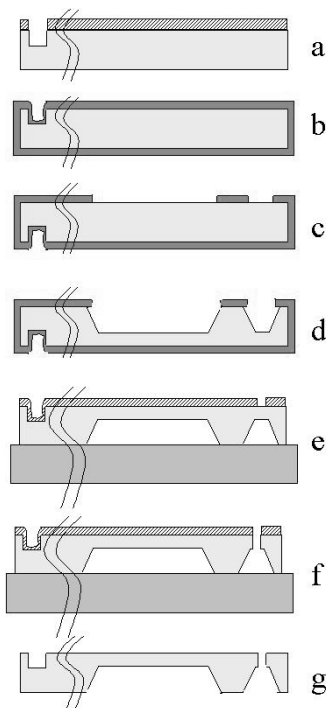Fig. 9.   Convex corner compensating structure (CCCS).

Fig. 10.   Fabrication process flow for convex element wafer.

Fig. 11.   Fabrication process flow for concave element wafer.

Fig. 12.   Convex feature: Pyramid on cantilever's tip.

was coupled and not removed, while its position was measured many times. Fig. 16 shows the nomenclature used for the wafer level experiment results and describes how repeatability, accuracy, error vector magnitude and error vector repeatability were calculated.

Table VI shows the results of a 20-cycle assembly and disassembly sequence, where all 96 cantilever/pyramid elements are used. The grooves showed signs of wear after many dozens of
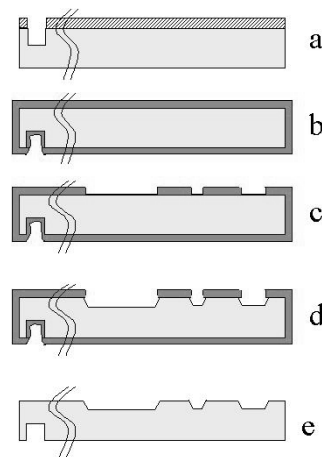
Fig. 13.   Array of convex structures.

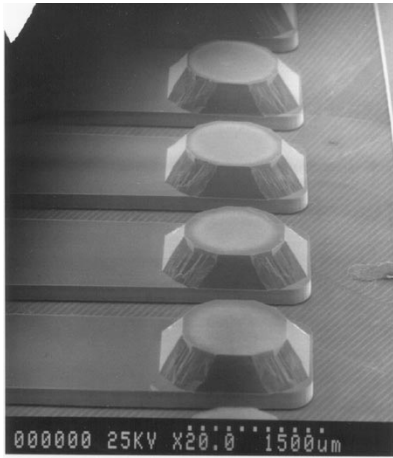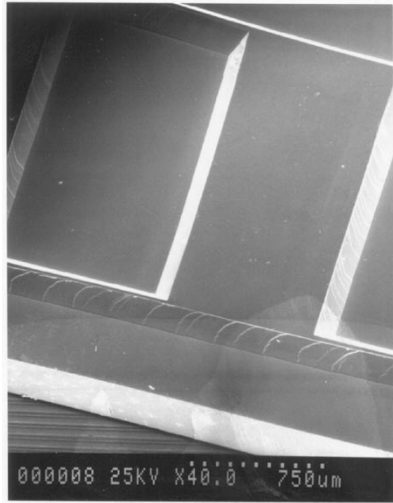Fig. 14.   Array of concave structures (notice bosses and v-trenches).
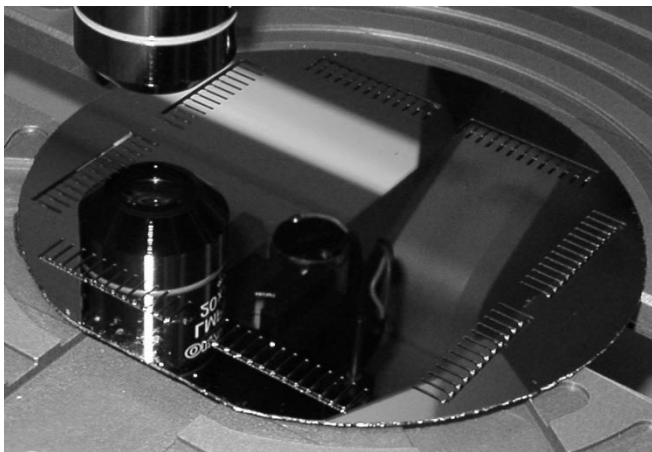

Fig. 15.   Testing of the passively mechanically aligned wafers. Notice wafer with convex features lies at the bottom.
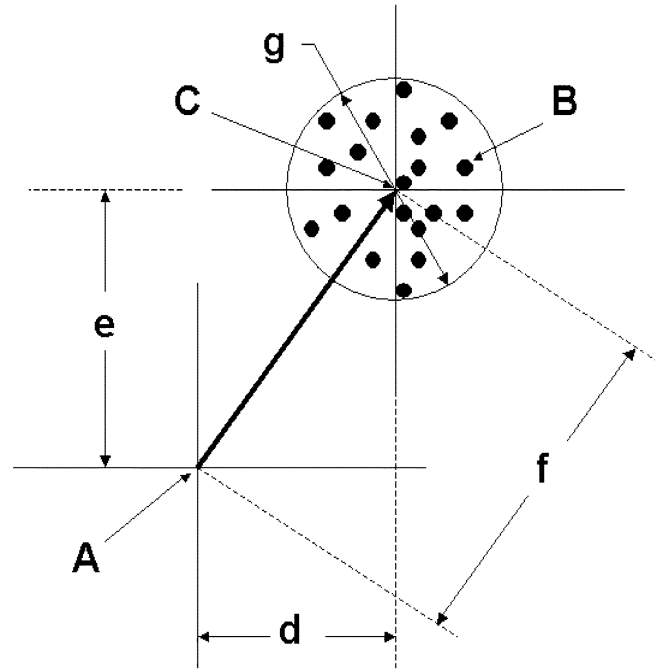

Fig. 16.   Nomenclature used for wafer level experiments: (a) bottom wafer alignment mark position (BWAM) used as reference; (b) top wafer alignment mark position (TWAM) at a particular assembly cycle; (c) average position of all TWAM (accuracy); (d), (e) accuracy in X and Y direction; (f) error vector magnitude; and (g) repeatability. The repeatability in X and Y is taken as the range of TWAM data in each direction, respectively. The error vector repeatability is calculated as the range of the magnitude of the error vectors.

TABLE V
PERFORMANCE OF THE TBM8 WAFER ALIGNMENT MEASUREMENT
SYSTEM, AS DETERMINED WITH "CAP TEST"

	ΔX (μm)	ΔY (μm)	Error (μm)
Accuracy	0.36	-5.31	5.33
Repeatability	0.42	0.42	0.42

however, it was felt that with the form of Fig. 17(a), if the desired performance was achieved, then the form of Fig. 17(c) could ultimately be used which would increase the baseline distance, thus increasing accuracy further, and requiring less valuable wafer space to be consumed by the coupling mechanism.

During this experiment, repeatability and accuracy were measured as a function of the number of engaged features. Submicrometer repeatability was achieved with as little as 8 mating features. Table VII shows repeatability and accuracy as a function of the number of engaged features. The offset between repeatability and accuracy is assumed to be caused by misalignment of the masks used to pattern the structures. This misalignment is a fraction of the minimum 20 μm feature size of the masks made from emulsion transparencies. The data shows that the use of many features does not necessarily provide a great increase in accuracy or repeatability as might be expected, but such increases are expected when there are random errors in the elements. The accuracy error is hypothesized to be systematic in the alignment fiducials, and the repeatability even with only 8 features (two per side) is very good; hence we conclude that wafers can be mechanically aligned to each other using just two

couplings, so a second set of wafers was used for experiments where the cantilevers were to be successively broken off starting at the corners and working inward as shown in Fig. 17(a). Intuition may seem to indicate that it would be better to work outward to end up with 8 cantilevers as shown in Fig. 17(b);
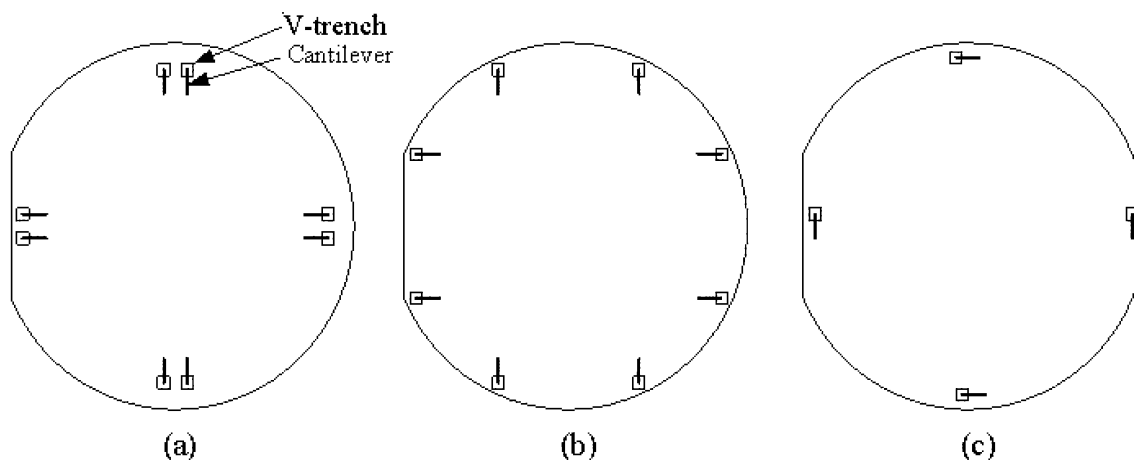
Fig. 17.   (a) The wafer coupling locations after the cantilevers were broken off. (b) An intuitive pattern that was not used. (c) The pattern that should be used as a result of measurements which showed excellent performance was obtained by (a).

TABLE VI
TEST RESULTS FOR WAFERS M-2 AND F-1 USING ALL
96 CANTILEVERS (CONTACTS)

	ΔX (μm)	ΔY (μm)	Error (μm)
Accuracy	0.88	-1.08	1.41
Repeatability	0.63	1.06	1.06

TABLE VII
TEST RESULTS (μm) FOR WAFERS M-2 AND F-2 AS A FUNCTION OF
REDUCING THE NUMBER OF CANTILEVERS (CONTACTS) FOR EACH TEST

	Total # of contacts	ΔX (μm)	ΔY (μm)	Error (μm)
Accuracy	96	-6.93	1.35	7.07
Repeatability	96	1.09	0.43	1.12
Accuracy	88	-6.26	0.75	6.3
Repeatability	88	0.84	0.78	0.87
Accuracy	80	-7.29	0.44	7.29
Repeatability	80	0.84	0.84	0.84
Accuracy	72	-1.68	4.52	4.83
Repeatability	72	-1.04	0.85	1.01
Accuracy	64	-4.3	-5.86	7.22
Repeatability	64	0.43	0.42	0.43
Accuracy	56	-5.99	-4.26	7.37
Repeatability	56	0.63	0.21	0.46
Accuracy	48	-6.55	-4.21	7.82
Repeatability	48	0.63	0.42	0.52
Accuracy	40	-6.46	-3.69	7.42
Repeatability	40	0.42	0.63	0.68
Accuracy	32	-4.61	-5.43	7.32
Repeatability	32	0.63	1.05	0.89
Accuracy	24	-7.56	-3.87	8.53
Repeatability	24	0.84	1.05	0.67
Accuracy	16	-7.51	-4.77	8.89
Repeatability	16	0.42	0.64	0.58
Accuracy	8	-7.14	-4.77	8.89
Repeatability	8	0.42	0.89	0.47

of these features per quadrant. This will minimally intrude on the useful wafer surface area.

VIII. CONCLUSIONS AND FUTURE WORK

The results of this work validate that it is possible to achieve submicron alignment of multiwafer assemblies, without the need for optical alignment hardware, using passive mechanical alignment features. Thus, this technique can have significant impact in multiwafer MEMS and stacked 3-D ICs. The present implementation does not work for anodic or fusion bonding applications, due to the KOH etch roughness, unless SOI wafers were used. However, we are pursuing design modifications to simplify the design.

Specifically, it is hypothesized that the pyramid structure could also alternatively be formed by an appropriate metal structure, formed by plating for example, that would protrude form the surface of a polished wafer and mate with annular structures made by DRIE to form essentially the same type of interface used by LEGOs; hence stacks of wafers aligned (coupled) in this manner could then be fusion bonded. In addition, the metal protrusions could be made as surfaces of revolution, which should increase accuracy by reducing edge contacts.

Furthermore, the requirement for tapping the wafers to ensure that the alignment elements properly engage needs to be studied. Future tests will be done to determine repeatability as a function of vibration direction, amplitude and duration.

REFERENCES

[1] J.-Q. Lü *et al.*, "Stacked chip-to-chip interconnections using wafer bonding technology with dielectric bonding glues," in *Proc. Interconnect Technology Conference, 2001*, Proc IEEE 2001 Int., 2001, pp. 219–221.
[2] A. R. Mirza, "One micron precision, wafer-level aligned bonding for interconnect, MEMS and packaging applications," in *Proc. Electronic Components & Technology Conference, 2000*, 2000 Proceedings 50th, 2000, pp. 676–680.
[3] Y. Bäcklund, "Micromechanics in optical microsystems-with focus on telecom systems," *J. Micromech. Microeng*, vol. 7, pp. 93–98, 1997.

[4] C. Strandman *et al.*, "Passive and fixed alignment of devices using flexible silicon elements formed by selective etching," *J. Micromech. Microeng.*, vol. 8, pp. 39–44, 1998.

[5] R. M. Bostock *et al.*, "Silicon nitride microclips for the kinematic location of optic fibers in silicon v-shaped grooves," *J. Micromech. Microeng.*, vol. 8, pp. 343–360, 1998.

[6] R. L. Smith *et al.*, "A wafer-to-wafer alignment technique," *Sens. Actuators*, vol. 20, pp. 315–316, 1989.

[7] L.-S. Huang *et al.*, "MEMS packaging for micro mirror switches," in *Proc. 48th Electronic Components & Technology Conference*, Seattle, WA, May 1998, pp. 592–597.

[8] B. R. Martin *et al.*, "Self-alignment of patterned wafers using capillary forces at a water-air interface," *J. Adv. Funct. Mater.*, vol. 11, no. 5, pp. 381–386, Oct. 2001.

[9] C. Evans, *Precision Engineering: An Evolutionary View*. Cranfield, U.K.: Cranfield Press, 1989, pp. 22–33.

[10] A. Slocum, *Precision Machine Design*. Dearborn, MI: SME, 1992, pp. 352–354.

[11] R. S. Whipple, "The design and construction of scientific instruments," *Trans. Opt. Soc.*, vol. 22, pp. 3–52, 1920–1921.

[12] L. S. Brooks, "Adjustable instrument mount," *J. Opt. Soc. Amer.*, vol. 44, p. 87, 1954.

[13] E. Hog, "A kinematic mounting," *Astron. Astrophys.*, vol. 41, pp. 107–109, 1975.

[14] A. Slocum, "Design of three-groove kinematic couplings," *Precis. Eng.*, vol. 14, no. 2, pp. 67–76, April 1992.

[15] P. Smeichen and A. Slocum, "Analysis of kinematic systems: A generalized approach," *Precis. Eng.*, vol. 19, no. 1, pp. 11–18, July 1996.

[16] C. H. Schouten, J. N. Rosielle, and P. H. Shellens, "Design of a kinematic coupling for precision applications," *Precis. Eng.*, vol. 20, no. 1, pp. 46–52, 1997.

[17] K. Autumn, Y. Liang, W. P. Chan, T. Hsieh, R. Fearing, T. W. Kenny, and R. Full, "Dry adhesive force of a single gecko foot-hair," *Nature*, vol. 405, pp. 681–685, 2000.

[18] A. Slocum, "Precision machine design: Macromachine design philosophy and its applicability to the design of micromachines," in *Proc. IEEE Micro Electro Mechanical Systems '92*, Travemunde, Germany, Feb. 4–7, 1992, pp. 37–42.

[19] H. Han, L. Weiss, and M. Reed, "Micromechanical velcro," *J. Microelectromech. Syst.*, vol. 1, pp. 37–43, Mar. 1992.

[20] G. K. Christiansen, "Toy Building Brick," U.S. Pat. 3 005 282, Oct. 1961.

[21] A. Slocum, D. Braunstein, and L. Muller, "Flexural Kinematic Couplings," U.S. Pat. 5,678, 944, Oct. 1997.

[22] M. Balasubramaniam, H. Dunn, E. Golaski, S. Son, K. Sriram, and A. Slocum, "An anti backlash two-part shaft with interlocking elastically averaged teeth," *Precis. Eng.*, vol. 26, no. 3, pp. 314–330, 2002.

[23] Q. Zhang *et al.*, "A new approach to convex corner compensation for anisotropic etching of (100) Si in KOH," *Sens. Actuators*, vol. A 56, pp. 251–254, 1996.

Alexander H. Slocum received the Ph.D. degree from the Massachusetts Institute of Technology (MIT), Cambridge, while simultaneously working from 1983 to 1985 at the National Bureau of Standards, where he also earned 12 superior service awards and a Department of Commerce Bronze Medal.

He is currently a Professor of Mechanical Engineering at MIT and a MacVicar Faculty Fellow. He has five dozen patents issued/pending and he designs manufacturing equipment for the automotive, aerospace, semiconductor, and entertainment industries. He has been involved in several manufacturing equipment company start-ups, and he has helped many different companies bring many different machines to the marketplace. In addition, he has also been involved with nine products that have been awarded R&D 100 awards, each for annually being one of one hundred most technologically significant new products. His research has involved three dozen Ph.D. students, and he is the recipient of the Society of Manufacturing Engineer's Frederick W. Taylor Research Medal. His current research interests focus on the development of instruments, MEMS, and nanotechnology.

Alexis C. Weber received the B.S. degree in mechanical and electrical engineering from Instituto Tecnologico y de Estudios Superiores de Monterrey (ITESM-CEM), Mexico, and the M.S. degree in mechanical engineering from the Massachusetts Institute of Technology (MIT), Cambridge, in 2002. He is currently pursuing the Ph.D. degree at MIT.

From 1999 to 2003, he worked for Delphi Corporation designing actuators for automotive applications. He has six patents pending and is author of two defensive publications. His research interests include precision machine design as well as design, fabrication and characterization of MEMS.